PROCEEDINGS OF SCIENCE

VCS and generalized polarizabilities from Mainz and JLab: Overview and new results

Nikos Sparveris[a,*]

[a] *Temple University,*
1925 N. 12th Street, Philadelphia, PA 19122, USA

E-mail: sparveri@temple.edu

The Generalized Polarizabilities (GPs) are fundamental properties of the nucleon. They characterize the nucleon's response to an applied electromagnetic field, giving access to the polarization densities inside the nucleon. As such they represent a central path towards a complete understanding of the nucleon dynamics. Previous measurements have challenged the theoretical predictions, raising questions in regard to the underlying mechanism responsible for a local enhancement of the electric GP at intermediate four-momentum transfer squared. The measurement of the magnetic GP, on the other hand, promises to quantify the interplay of the paramagnetic and the diamagnetic contributions inside the proton. An overview and recent efforts on the front of the proton GPs are discussed.

The 10th International Workshop on Chiral Dynamics - CD2021
15-19 November 2021
Online

*Speaker

PoS(CD2021)076

1. Introduction

The polarizabilities of a composite system such as the nucleon [1] are fundamental structure constants and can be accessed experimentally by Compton scattering processes. In real Compton scattering, the incoming real photon offers the nucleon deformation and by measuring the energy and angular distributions of the outgoing photon we can determine the magnitude of the nucleon polarizabilities. Although the electric, magnetic and some of the spin polarizabilities are known with reasonable accuracy from Compton scattering experiments, we have limitted information about the distribution of polarizability density inside the nucleon. We can gain access to this information through the virtual Compton scattering (VCS) process where the incident real photon is replaced by a virtual photon [2]. The virtuality of the photon offers access to the spatial distribution of the polarization densities. The momentum of the outgoing real photon q' sets the scale of the EM perturbation while the momentum of the virtual photon q sets the scale of the observation. In analogy to the form factors for elastic scattering, which describe the charge and magnetization distributions, VCS gives access to the deformation of these distributions under the influence of an electromagnetic field perturbation as a function of the distance scale. The structure dependent part of the process is parametrized by the Generalized Polarizabilities (GPs) which can be seen as Fourier transforms of local polarization densities (electric, magnetic, and spin) [3]. The GPs are therefore a probe of the nucleon dynamics, allowing us, e.g., to study the role of the pion cloud and quark core contributions to the nucleon dynamics at various length scales.

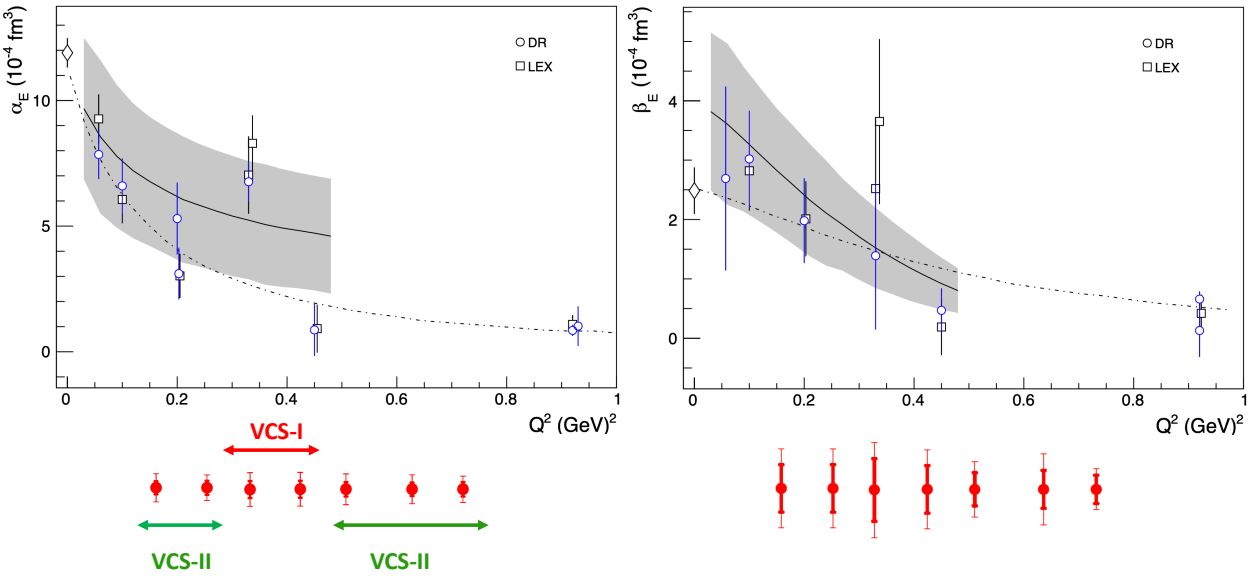

Figure 1: World data [4, 5, 7–9, 11–13] (open symbols) for α_E and β_M. The kinematic ranges for the VCS-I (E12-15-001) experiment [5] (data analysis in progress) and for the VCS-II (experimental proposal in preparation) are marked with the horizontal arrows. The projected measurements for VCS-I and VCS-II are shown with solid red points. The solid curve shows the ChEFT calculation of [46]. The dash-dot curve shows the DR prediction assuming a pure dipole fall-off for both scalar GPs.

The proton electric polarizability α_E [6] is much smaller than the volume scale of a nucleon e.g. contrary to the atomic polarizabilities which are of the size of the atomic volume. Its small

size reveals the stiffness of the proton as a direct consequence of the strong binding of its inner constituents, the quarks and gluons and underlines the intrinsic relativistic character of the nucleon. In recent theoretical models, the electric GP α_E is predicted to decrease monotonically with Q^2. The smallness of the magnetic GP β_M [6] relative to α_E can be explained by the existence of the competing paramagnetic and diamagnetic contributions, which nearly cancel. The β_M is predicted to go through a maximum before decreasing. This feature is typically explained by the dominance of diamagnetism due to the pion cloud at long distance, or small Q^2, and the dominance of paramagnetism due to a quark core at large Q^2.

A series of early VCS experiments [7–11] (see Fig. 1) offered a first exploration of the scalar GPs of the proton. The first experimental evidence contradict the naive Ansatz of a single-dipole fall-off for α_E as a function of Q^2. They point out to an enhancement at low Q^2 which is evidenced by two independent experiments [7, 8]. This unexpected structure is not understood and a variety of processes are candidates to explain this behavior. The α_E anomaly has been considered with reservation for nearly two decades, based on the absence of an independent experimental confirmation, the relatively large experimental uncertainty and the theory being unable to describe such a feature. The experimental study of the magnetic polarizability on the other hand, when accomplished with sufficient precision, can enable a better understanding of the competing processes manifesting in the interplay between diamagnetism and paramagnetism in the proton. In regards to the theory, the GPs have been calculated by various approaches, i.e. Heavy Baryon Chiral Perturbation Theory (HBChPT) [14–18], Dispersion Relations (DR) [20, 21], Constituent Quark models [22–24], Linear Sigma model [25, 26] and Effective Lagrangian [27, 28]. None of the calculations is able to describe the observed structure of α_E, as they all predict a smooth fall-off as a function of Q^2. Recently, the developed formalism to extract light-front quark charge densities from nucleon form factor data was extended to the deformations of these quark charge densities when applying an external electric field [3, 33]. This in-turn allows for the concept of GPs to be used to describe the spatial deformation of the charge and magnetization densities, as described in [31]. The suggested α_E enhancement at intermediate Q^2 will result to a spatial distribution of the induced polarization that extends noticeably to larger transverse distances [31]. High precision ongoing measurements at the low and intermediate Q^2 regime will allow to pin down this large distance structure.

2. Recent results and ongoing efforts

An experiment at MAMI recently concluded its effort and new results for both the scalar GPs were published. The measurements focused in the region around the kinematics of the previously reported $\alpha_E(Q^2)$ anomaly [7, 8] (but not on the exact same kinematics), namely at three kinematical settings: $Q^2 = 0.1\ GeV^2$, $0.2\ GeV^2$ and $0.45\ GeV^2$. The experiment reported a smooth and rapid fall-off with Q^2 [12, 13], as shown in Fig. 1. Thus, the results of this experiment indicated some tension with the earlier reported measurements at $Q^2 = 0.33\ GeV^2$ [7, 8].

A new experimental effort [5] is currently ongoing at the Thomas Jefferson National Accelerator Facility. The experiment acquired data in 2019 and accessed the VCS reaction in the region $Q^2 = 0.27\ GeV^2$ to $0.43\ GeV^2$. In this region, both of the scalar GPs are particularly sensitive to the nucleon dynamics. The experiment took advantage of the unique capabilities of the Hall

C setup at Jefferson Lab, exploited the fact that the polarizabilities are sensitive to the excited spectrum of the nucleon (e.g. unlike the nucleon elastic form factors that describe only the ground state) and promises to study the anomalous behaviour of $\alpha_E(Q^2)$ with VCS measurements of unprecedented precision. Conducting the measurements in the resonance region - as opposed to the pion threshold region where earlier measurements [7, 8] were performed - offers enhanced sensitivity to the polarizabilities. Moreover, in addition to the VCS cross section, the experiment targeted the in-plane azimuthal asymmetry of the VCS cross section with respect to the momentum transfer direction, $A_{(0,\pi)}$, where

$$A_{(\phi_{\gamma^*\gamma}=0,\pi)} = \frac{d\sigma^5_{\phi_{\gamma^*\gamma}=0} - d\sigma^5_{\phi_{\gamma^*\gamma}=\pi}}{d\sigma^5_{\phi_{\gamma^*\gamma}=0} + d\sigma^5_{\phi_{\gamma^*\gamma}=\pi}}. \tag{1}$$

The $\phi_{\gamma^*\gamma}$ refers to the angle between the plane of the two (incoming and scattered) electrons and the photon-proton plane. The asymmetry enhances the sensitivity in $\alpha_E(Q^2)$ and allows for part of the systematic uncertainties to be suppressed. Furthermore, in parallel to the ep→epγ reaction, the ep→epπ^0 reaction was simultaneously measured in the spectrometer acceptance. The pion electroproduction cross section is well known in this region and offers a stringent, real-time normalization control to the measurement of the ep→epγ reaction.

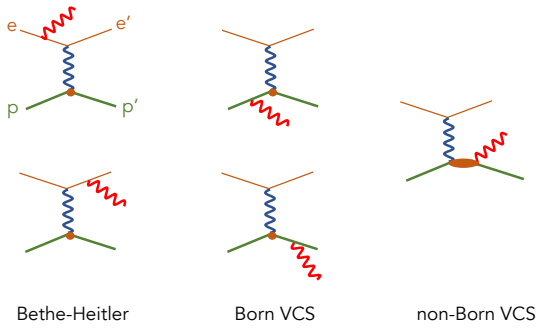

Figure 2: The mechanisms contributing to ep→epγ. The small circles represent the interaction vertex of a proton with a virtual photon and the ellipse the non-Born VCS amplitude.

The data were acquired in Hall C of Jefferson Lab during experiment E12-15-001. Electrons with energies of 4.56 GeV at a beam current up to 20 μA were produced by Jefferson Lab's Continuous Electron Beam Accelerator Facility (CEBAF) and were scattered from a 10 cm long liquid-hydrogen target. The Super High Momentum Spectrometer (SHMS) and the High Momentum Spectrometer (HMS) of Hall C were used to detect in coincidence the scattered electrons and recoil protons, respectively. The two spectrometers are equipped with similar detector packages, including a set of scintillator planes, that were used to form the trigger and to provide time-of-flight information, and a pair of drift chambers used for tracking. The time-of-flight in the HMS spectrometer was used for the proton identification and the SHMS Pb-glass calorimeter was used for the electron identification. The coincidence time was determined as the difference in the time-of-flight between the two spectrometers, accounting for path-length variation corrections from the central trajectory and for the individual start-times. The experimental setup offered a $\sim$ 1 ns (FWHM) resolution in the coincidence timing spectrum. The random coincidences were subtracted using

the accidental bands of the coincidence time spectrum. The VCS events were identified from the missing-mass reconstruction, through a selection cut around the photon peak in the missing-mass-squared spectrum. The missing mass and the coincidence time-of-flight spectra are shown in Fig. 3. Data were taken with an empty target in order to account for the background contributions from the target walls. Elastic scattering measurements with a proton target were performed throughout the experiment for calibration and normalization studies. The measurement of the absolute cross section, $d^5\sigma/dE'_e d\Omega'_e d\Omega_{cm}$, requires the determination of the five-fold solid angle, where dE'_e, $d\Omega'_e$ the differential energy and solid angle of the scattered electron in the laboratory frame and $d\Omega_{cm}$ is the differential solid angle of the emitted photon in the center-of-mass (c.m.). The experimental acceptance has been calculated by using the simulation program, SIMC, that integrates the beam configuration, target geometry, spectrometer acceptances, resolution effects, energy losses and radiative corrections. A sub-set of the preliminary cross section results is presented in Fig. 4. The measurements cover a wide range of c.m. polar angle of the real photon with respect to the virtual photon direction, $\theta_{\gamma^*\gamma}$ and avoid the kinematics dominated by the BH-process where the polarizability effect is suppressed.

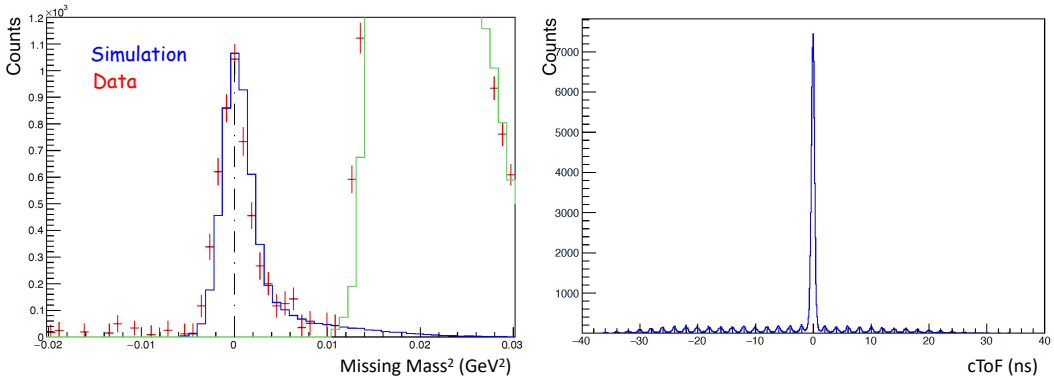

Figure 3: Missing mass squared spectrum and coincidence time-of-flight spectrum from the E12-15-001 experiment at Jefferson Lab.

The measured cross section of the $ep \rightarrow ep\gamma$ reaction receives contributions from the photon that is emitted by either the lepton, known as the Bethe-Heitler (BH) process, or by the proton, the fully virtual Compton scattering (FVCS) process, as shown in Fig. 2. The FVCS amplitude is decomposed into a Born contribution, with the intermediate state being the nucleon, and a non-Born contribution that carries the physics of interest and is parametrized by the GPs. The BH and the Born-VCS contributions are well known, entirely calculable in terms of the proton electromagnetic form factors. The GPs can be extracted from the measured cross sections through a fit that employs the dispersion relations (DR) model for VCS [19, 20]. In the DR formalism, the two scalar GPs come as an unconstrained part and can be adjusted as free parameters, while the proton electromagnetic form factors are introduced as an input. In this procedure, the experimental cross sections are compared to the DR model predictions for all possible values for the two GPs, and the $\alpha_E(Q^2)$ and $\beta_M(Q^2)$ are fitted by a χ^2 minimization. Preliminary results for the cross sections and the scalar GPs have been extracted from the experimental measurements and the data analysis is currently ongoing.

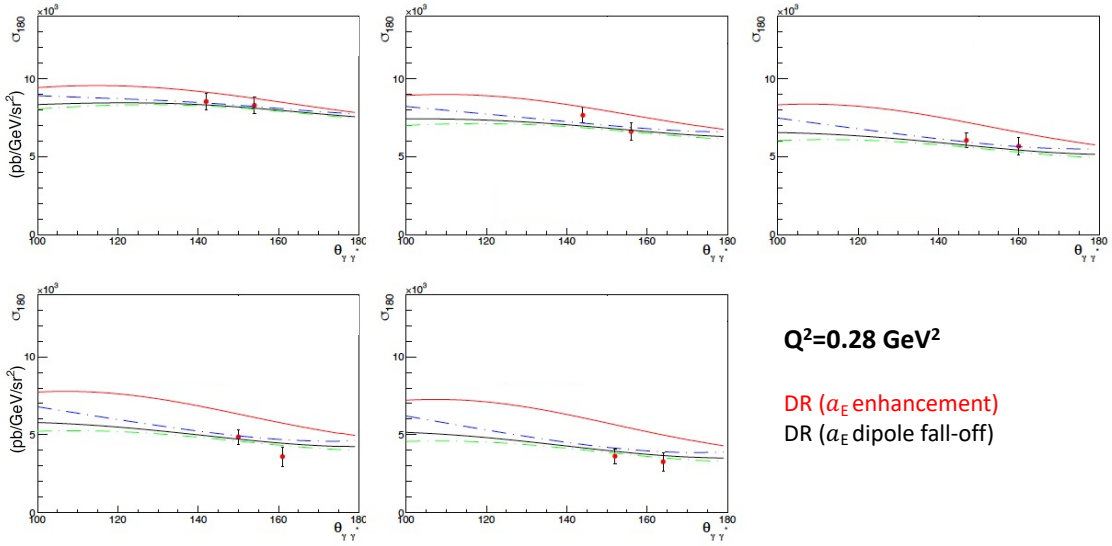

Figure 4: Preliminary cross section results from the E12-15-001 experiment at $Q^2 = 0.28\ GeV^2$ for in-plane kinematics. The red and black curves correspond to the DR calculation assuming an enhancement to the electric GP (consistent with the early MAMI results at $Q^2 = 0.33\ GeV^2$) and a dipole fall-off for the electric GP, respectively. The blue and green curves show the sensitivity to the magnetic GP at these kinematics, for different values of the mass scale parameter Λ_b ranging from 0.1 to 0.9. The panels starting from left-to-right (and top-to-bottom) correspond to W bins from W=1230 MeV to W=1270 MeV.

3. Future prospects

The data analysis of the E12-15-001 experiment is at an advanced stage and will be completed in the upcoming months. At that point, the electric and magnetic GPs will be extracted at three Q^2 points within the region of $Q^2 = 0.27\ GeV^2$ to $0.43\ GeV^2$. The experiment will offer a nearly factor of 2 improvement in the uncertainty of these measured GPs in that region. The projected measurements are shown in Fig. 1. Once these results become available, it will become possible to derive the spatial deformation of the quark distributions in the proton, subject to the influence of an external electromagnetic field [31]. The spatial density can be formulated by considering the proton in the light-cone frame. The extraction of the spatial deformation of the quark densities from the measured GPs is effectively an extension of the formalism to extract the light-front quark charge densities from the proton form factor data. First, a precise Q^2-parametrization of the scalar GPs will be derived from a fit to the experimental data and from that the induced polarization in the proton will be extracted following [31]. A primary measure that quantifies the extension of a spatial distribution is the mean square radius. The mean square electric polarizability radius of the proton $\langle r^2_{\alpha_E} \rangle$ is related to the slope of the electric GP at $Q^2 = 0$

$$\langle r^2_{\alpha_E} \rangle = \frac{-6}{\alpha_E(0)} \cdot \frac{d}{dQ^2} \alpha_E(Q^2) \Big|_{Q^2=0}. \tag{2}$$

The mean square electric polarizability radius $\langle r^2_{\alpha_E} \rangle$ will be extracted by determining the slope of $\alpha_E(Q^2)$ at $Q^2 = 0$ from the fit to the world-data, while for $\alpha_E(0)$ the PDG value [48] will be

adopted.

As the E12-15-001 data analysis is converging, work has began on the preparation of the proposal for the VCS-II experiment at JLab, following the recommendation of the JLab PAC44 report. The VCS-I preliminary results show evidence for a local enhancement of the electric GP in the measured region and improve significantly the precision of the extracted GPs. It now becomes important to map the Q^2-dependence of the GPs with more detail, so that the underlying dynamics responsible for this anomalous behaviour can be decoded. The range and projected measurements for VCS-II are shown in Fig. 1. The proposal will be submitted to the JLab PAC in summer 2023.

A future prospect involves the study of the VCS process at low energies with experiments that utilize positron beams. By using unpolarized electron and positron beams one can measure the unpolarized beam-charge asymmetry A^C_{UU}, while with polarized lepton beams one can access the lepton beam-spin asymmetry A^e_{LU} [49]. The sensitivity of the asymmetries to the GPs is significant around the $\Delta(1232)$ resonance region, both for in-plane and for out-of-plane kinematics. A research program that will involve asymmetry measurements with positron and electron beams can offer a complementary path to access the proton GPs and to further improve their precision. Studies to develop such a research program are currently ongoing.

Lastly, a fertile line for the study of the nucleon structure is offered through the measurement of the spin polarizabilities of the proton that describe the coupling of the proton spin with an applied electric or magnetic field. The internal spin structure of the nucleon appears at third order in the energy expansion of the Compton scattering amplitude, where one can identify four independent spin polarizabilities. Experimental measurements of the spin GPs are difficult and challenging. The first VCS experiment with double polarization was done at MAMI [44]. Using a polarized electron beam and measuring the recoil proton polarization, a double polarization asymmetry is built. This experiment showed less sensitivity than expected, and only one new structure function which is a linear combination of scalar and spin GPs could be extracted [44]. An alternative path can be followed to access the (pure spin) structure function P_{TT}, by measuring the $(P_{LL} - P_{TT}/\epsilon)$ structure function in an unpolarised experiment, and making a separation of P_{LL} and P_{TT} . This requires measurements at high and low ϵ, i.e. a Rosenbluth-type technique. At JLab one could perform such an experiment in Hall C (with the SHMS and the HMS spectrometers) or in Hall A (with the two HRS spectrometers). Plans to develop such an experimental program are currently underway.

References

[1] F. Hagelstein, R. Miskimen and V. Pascalutsa, Prog. Part. Nucl. Phys. 88 (2016) 29-97

[2] P. A. M. Guichon and M. Vanderhaeghen, Prog. Part. Nucl. Phys. **41**, 125 (1998).

[3] M. Gorchtein, C. Lorc´e, B. Pasquini, M. Vanderhaeghen, Phys.

[4] A. Blomberg et al., Eur. Phys. J. A 55 (2019) 10, 182

[5] *Measurement of the Generalized Polarizabilities of the Proton in Virtual Compton Scattering*, N. Sparveris et al., Jefferson Lab Proposal PR12-15-001; https://www.jlab.org/exp_prog/proposals/16/C12-15-001.pdf

Rev. Lett. 104, 112001 (2010)

[6] V. Olmos de Leon, et al., Eur. Phys. J. A10 (2001) 207

[7] J. Roche, et al., Phys. Rev. Lett. 85 (2000) 708-711.

[8] P. Janssens, et al., Eur. Phys. J. A37 (2008) 1-8

[9] G. Laveissiere, et al., Phys. Rev. Lett. 93 (2004) 122001

[10] H. Fonvieille, et al., Phys. Rev. C86 (2012) 015210

[11] P. Bourgeois, et al., Phys. Rev. Lett. 97 (2006) 212001

[12] J. Beričič, et al., Phys. Rev. Lett. 123 (2019) 192302

[13] H. Fonvieille, et al., Phys. Rev. C 103 (2021) 025205

[14] T. R. Hemmert, B. R. Holstein, G. Knochlein, S. Scherer, Phys. Rev. D55 (1997) 2630-2643.

[15] T. R. Hemmert, B. R. Holstein, G. Knochlein, S. Scherer, Phys. Rev. Lett. 79 (1997) 22-25.

[16] T. R. Hemmert, B. R. Holstein, G. Knochlein, D. Drechsel, Phys. Rev. D62 (2000) 014013.

[17] C. W. Kao, M. Vanderhaeghen, Phys. Rev. Lett. 89 (2002) 272002.

[18] C.-W. Kao, B. Pasquini, M. Vanderhaeghen, Phys. Rev. D70 (2004) 114004.

[19] B. Pasquini, D. Drechsel, M. Gorchtein, A. Metz, and M. Vanderhaeghen, Phys. Rev. C 62, 052201(R),(2000).

[20] B. Pasquini, M. Gorchtein, D. Drechsel, A. Metz, M. Vanderhaeghen, Eur. Phys. J. A11 (2001) 185-208.

[21] D. Drechsel, B. Pasquini, M. Vanderhaeghen, Phys. Rept. 378 (2003) 99-205.

[22] P.A.M. Guichon, G.Q. Liu and A.W. Thomas, Nucl. Phys. A 591 (1995) 606.

[23] G. Q. Liu, A. W. Thomas, P. A. M. Guichon, Austral. J. Phys. 49 (1996) 905-918.

[24] B. Pasquini, S. Scherer, D. Drechsel, Phys. Rev. C63 (2001) 025205.

[25] A. Metz, D. Drechsel, Z. Phys. A356 (1996) 351-357.

[26] A. Metz, D. Drechsel, Z. Phys. A359 (1997) 165-172.

[27] M. Vanderhaeghen, Phys. Lett. B368 (1996) 13-19.

[28] A. Y. Korchin, O. Scholten, Phys. Rev. C58 (1998) 1098-1100.

[29] V. Lensky, V. Pascalutsa, M. Vanderhaeghen, Eur. Phys. J. **C 77**,(2017) no.2, 119.

[30] A. Korchin and O. Scholten, Phys. Rev. C58 (1998) 1098

[31] M. Gorchtein, C. Lorce, B. Pasquini, M. Vanderhaeghen, Phys. Rev. Lett. 104, 112001 (2010).

[32] W. Detmold, B. Tiburzi, A. Walker-Loud, Phys. Rev. D 81, 054502 (2010)

[33] A.I. Lvov, S. Scherer, B. Pasquini, C. Unkmeir, D. Drechsel, Phys. Rev. C 64, 015203 (2001)

[34] B. Pasquini, D. Drechsel, and M. Vanderhaeghen, Eur. Phys. J. Special Topics 198, 269285 (2011)

[35] *Proposed experiment to study the nucleon structure by measurement of Virtual Compton Scattering in the* Δ *resonance at MAMI*, N. Sparveris et al., MAMI A1 proposal (2011); http://quarks.temple.edu/~sparveri/MAMI-A1-VCS-Delta-proposal.pdf

[36] K. I. Blomqvist, et al., Nucl. Instrum. Meth. A403 (1998) 263-301

[37] Spin 2018, 23rd International Spin Symposium, Ferrara, Italy, September 2018

[38] ECT* Workshop Nucleon Spin Structure at Low-Q: A Hyperfine View, Trento, Italy, July 2018

[39] Hadron 2017, Salamanca, Spain, September 2017

[40] WWND 2017, Winter Workshop on Nuclear Dynamics, Utah, January 2017

[41] N. Sparveris et al., Jefferson Lab proposal E-08-010

[42] https://www.jlab.org/Hall-C/upgrade/

[43] https://www.jlab.org/Hall-C/equipment/HMS.html

[44] L. Doria et al., Phys. Rev. C92 (2015) no.5, 054307.

[45] M. Vanderhaeghen et al. *Phys. Rev. C* **62**, 025501 (2000).

[46] V. Lensky, V. Pascalutsa, M. Vanderhaeghen *Eur. Phys. J. C* **77**, 119 (2017).

[47] H. Fonvieille, B. Pasquini and N. Sparveris, Prog. Part. Nucl. Phys. 113 (2020) 103754.

[48] P.A. Zyla *et al.* Review of Particle Physics. *Prog. Theor. Exp. Phys.* **2020**, 083C01 (2020).

[49] B. Pasquini and N. Vanderhaeghen, Eur. Phys. J. A 57 (2021) 11, 316.